Effects of Intermediate Filaments on Actin-Based Motility of *Listeria monocytogenes*

Paula A. Giardini* and Julie A. Theriot†
Departments of *Biochemistry and †Microbiology and Immunology, Stanford University School of Medicine, Stanford, California 94305 USA

ABSTRACT How does subcellular architecture influence the intracellular movements of large organelles and macromolecular assemblies? To investigate the effects of mechanical changes in cytoplasmic structure on intracellular motility, we have characterized the actin-based motility of the intracellular bacterial pathogen *Listeria monocytogenes* in normal mouse fibroblasts and in fibroblasts lacking intermediate filaments. The apparent diffusion coefficient of *L. monocytogenes* was two-fold greater in vimentin-null fibroblasts than in wild-type fibroblasts, indicating that intermediate filaments significantly restrict the Brownian motion of bacteria. However, the mean speed of *L. monocytogenes* actin-based motility was statistically identical in vimentin-null and wild-type cells. Thus, environmental drag is not rate limiting for bacterial motility. Analysis of the temporal variations in speed measurements indicated that bacteria in vimentin-null cells displayed larger fluctuations in speed than did trajectories in wild-type cells. Similarly, the presence of the vimentin meshwork influenced the turning behavior of the bacteria; in the vimentin-null cells, bacteria made sharper turns than they did in wild-type cells. Taken together, these results suggest that a network of intermediate filaments constrains bacterial movement and operates over distances of several microns to reduce fluctuations in motile behavior.

INTRODUCTION

Cytoplasmic architecture in eukaryotic cells is highly complex and inhomogeneous. A variety of membrane-bound organelles and large-scale macromolecular assemblages navigate a space scaffolded by cytoskeletal networks including actin filaments, microtubules, and intermediate filaments. Whereas small molecules diffuse rapidly in cytoplasm, with mobilities comparable to their mobilities in water, macromolecules with dimensions greater than a few nanometers are significantly constrained by these filamentous networks, and the effective viscosity they experience has a dramatically nonlinear dependence on their size (reviewed in Luby-Phelps, 2000). Movements of large macromolecular assemblies and membranous organelles within cells are also likely to be strongly affected by local geography, as cytoskeletal networks are nonuniform. In fibroblasts, for example, intermediate filament networks are densest near the nucleus, whereas structurally distinct actin-rich gels and webs predominate close to the plasma membrane.

The local organization and mechanical properties of cytoskeletal networks have been examined by studies of the mobility of tracer probes in living cells (Luby-Phelps et al., 1986, 1987; Luby-Phelps and Taylor, 1988; Luby-Phelps, 1994; Janson et al., 1996; Jones et al., 1997; Goulian and Simon, 2000). These studies and others using laser-tracking microrheology (Yamada et al., 2000) suggest, for example, that intermediate filament networks present a two- to four-fold impediment to diffusion of large probes (0.1–0.2 μm), particularly in the perinuclear region (Jones et al., 1997). However, very little information is available about the influence of cytoarchitecture on the mobility of objects the size of large organelles ($>$0.2 μm), in part because particles this large cannot be easily microinjected into cells. Furthermore, on longer time scales cytoplasm is probably viscoelastic rather than simply viscous. Thus, the inhomogeneous nature of cytoplasm makes it likely that organelles actively moving through cytoplasm will experience different drag effects than do passively diffusing probes, and the magnitude of the viscoelastic drag probably depends on the speed as well as size of the moving objects.

Listeria monocytogenes, a bacterial pathogen that lives and grows in the cytoplasm of infected host cells, is similar in size (1–2 μm) to certain large intracellular organelles such as mitochondria. After infection, it moves within and between host cells using a form of motility that is driven by the polymerization of actin in the shape of a comet tail closely associated with the bacterial surface (Tilney and Portnoy, 1989; Mounier et al., 1990). *L. monocytogenes* motility is well characterized. Over the past decade, all factors necessary and sufficient for its motility have been identified and described biochemically (Loisel et al., 1999; reviewed in Cameron et al., 2000). *L. monocytogenes* promises to be a useful probe of cytoarchitecture. First, it choreographs its own entry into cell cytoplasm, thereby obviating the need for microinjection. Second, because the viscoelastic properties of many materials are a function of not only the size, but also of the speed, of the probe used to characterize them, actin-propelled *L. monocytogenes* is a kinematic probe that can explore all regions of the cell

Received for publication 18 June 2001 and in final form 18 September 2001.

Address reprint requests to Dr. Julie A. Theriot, Department of Biochemistry, Stanford University School of Medicine, 279 West Campus Drive, Stanford, CA 94305-5307. Tel.: 650-725-7968; Fax: 650-723-6783; E-mail: theriot@cmgm.stanford.edu.

0006-3495/01/12/3193/11 $2.00

cytoplasm. Speed and persistence of movement of *L. monocytogenes* vary greatly in different host cell types (Dabiri et al., 1990; Theriot et al., 1992; Robbins et al., 1999) and in vitro systems (Theriot et al., 1994; Welch et al., 1997; David et al., 1998; May et al., 1999). These differences may be due in part to variations in the concentrations of proteins required for motility (Loisel et al., 1999) and in part due to structural and physical heterogeneities within the subcellular environment (Nanavati et al., 1994).

In this report, we have separated these two influences and specifically examined the effect of altering host cell cytoplasmic architecture on the actin-based movement of *L. monocytogenes*. We have found that Brownian motion of *L. monocytogenes* is two times greater in fibroblasts lacking intermediate filaments compared with Brownian motion in wild-type fibroblasts. However, this two-fold change in bacterial diffusivity has no effect on the mean speed of actin-based motility, suggesting that intracellular bacterial speed is not limited by cytoplasmic drag. Despite the negligible net change in speed, the intermediate filament network does impose a large-scale dampening effect on bacterial motility, significantly reducing fluctuations in speed and limiting turning. We find that the overall structural integration contributed to cytoplasm by intermediate filaments influences intracellular movements over distances of several microns.

MATERIALS AND METHODS

Bacterial culture and host cell infection procedures

MFT-6 (vimentin +/+) or MFT-16 (vimentin −/−) mouse 3T3 fibroblasts (Holwell et al., 1997) were generously provided by Dr. Robert Evans (University of Colorado Health Sciences Center, Boulder, CO). Cells were seeded onto collagen-coated coverslips in six-well tissue culture plates containing 2 ml of Dulbecco's modified Eagle's medium (DMEM) supplemented with 10% fetal bovine serum (FBS; Gibco, Gaithersburg, MD) and 1% antibiotic antimycotic (ABAM) (Gibco) 24 h before bacterial infection. *L. monocytogenes* strain 10403S (Bishop and Hinrichs, 1987) or DP-L1942 (Brundage et al., 1993) was grown in liquid BHI medium (Difco, Detroit, MI) for 12–15 h at room temperature without agitation. Bacteria were resuspended in 2 ml of DMEM containing 10% FBS, and 50–100 μl of the bacterial resuspension was added to fibroblast cultures and incubated at 37°C for 1 h. Infected fibroblasts were washed and resuspended in DMEM (10% FBS) with 50 μg/ml gentamicin (Sigma Chemical Co., St. Louis, MO).

Rhodamine-phalloidin staining of infected fibroblasts

Infected vimentin +/+ and vimentin −/− fibroblasts grown on coverslips were fixed at 5 h after infection with 2% paraformaldehyde in phosphate-buffered saline (PBS: 0.9 mM $CaCl_2$, 2.7 mM KCl, 1.5 mM KH_2PO4, 0.5 mM $MgCl_2$, 137 mM NaCl, and 8.0 mM Na_2HPO_4) for 5 min and permeabilized in extraction buffer containing 0.5% Triton X-100 detergent (0.5% Triton X-100, 10 mM Tris HCl, pH7.4, 120 mM NaCl, 75 mM KCl, 2 mM EDTA, 2 mM EGTA) for 10 min. Coverslips were incubated in block solution (PBS with 0.2% bovine serum albumin (BSA) and 1% FBS) for 30 min, washed with PBS, and then incubated with 0.4 U of rhodamine-phalloidin (Molecular Probes, Eugene, OR) in PBS for 30 min. Coverslips were washed again with PBS and mounted on slides in a 10% solution of 10 mM *p*-phenylenediamine, 1.0 mg/ml *n*-propylgallate in PBS with 90% glycerol. Fluorescence micrographs were captured on an Axioplan 2 microscope equipped with phase-contrast and epifluorescence optics (Carl Zeiss, Thornwood, NY) and a cooled CCD camera (Princeton Instruments (Princeton, NJ) Micromax back-illuminated frame transfer, 512 × 512 pixel chip size). Comet tails were observed using a 60× objective lens coupled with a 2× magnifying lens. Sixteen-bit digital images were captured using Metamorph software (version 3.5, Universal Imaging, Media, PA) and converted to eight-bit images in Adobe Photoshop (version 5.0.2, Adobe Systems, Tucson, AZ).

Phase-contrast video microscopy and bacterial tracking procedures

All video sequences of wild-type *L. monocytogenes* strain 10403S were collected between 6 and 8 h after infection. For measurements of diffusion coefficients, *L. monocytogenes* strain DP-L1942 (*actA*$^-$) (Brundage et al., 1993) was imaged within 3–5 h after infection. Coverslips containing infected fibroblasts were mounted in a temperature-controlled chamber and bathed in DMEM lacking phenol red with 10% FBS and 20 mM Hepes (Gibco). To prevent evaporation of media during imaging, a thin layer of silicone DC-200 oil (Fluka Chemika, Sigma-Aldrich, Steinheim, Switzerland) was added to cover the surface of media in the chamber. Time-lapse imaging of infected host cells was performed on a Nikon Diaphot-300 inverted microscope with an intensified charge-coupled device (ICCD) camera (Dage-MTI (Michigan City, IN) GenII Sys/CCD-c72) using Metamorph software (Universal Imaging). All infections and imaging were performed on at least three separate days for each condition tested.

For infections with *L. monocytogenes* strain 10403S, individual bacteria undergoing directed actin-based movement were tracked at their front tips using the track points function of Metamorph for each image in sequential order. For diffusive bacteria of *L. monocytogenes* strain DP-L1942 (*actA*$^-$), the center of each bacterium was tracked. Error in tracking was estimated for moving bacteria by tracking a single bacterium for 33 frames, calculating the speed at each interval, and repeating this procedure on the same individual track 10 times. The average variability in speed measured for each interval was 0.019 μm/s. The error in measured speed over the entire trajectory was estimated by calculating the standard deviation of the distribution of mean speed for the 10 independent tracking measurements (0.0004 μm/s).

Measurements of diffusion coefficient

Measurements of diffusion coefficients of *L. monocytogenes* DP-L1942 in live cells were made by tracking the center of individual bacteria from frame to frame in the video sequence. Movement along the longitudinal and orthogonal bacterial axes appeared random. For each trajectory consisting of 12–60 frames, the mean squared displacement MSD($n\Delta t$) was computed for all nonoverlapping consecutive pairs of values. Mean squared distances were calculated for 48 individual bacterial trajectories in vimentin +/+ fibroblasts and 51 trajectories in vimentin −/− fibroblasts. To determine the diffusion coefficient (D), a best-fit line was determined by least-squares analysis to MSD($n\Delta t$) where $1 \leq n \leq 10$ (Saxton, 1997). *L. monocytogenes* was approximated as an ellipsoid of length 2.0 μm and width 0.8 μm (F. Soo and J.A. Theriot, unpublished observation). D was calculated for two-dimensional diffusion (Berg, 1993; Qian et al., 1991).

Statistical analysis of bacterial velocity

For inter-track randomization analysis in Fig. 3, *C* and *D*, speed measurements for all bacteria in the vimentin +/+ or vimentin −/− populations

were pooled, and the order of the data points in the entire group was randomized. The randomized data points were then reassigned to individual bacterial trajectories of the same number and length as in the original data set. Intra-track randomization analysis (Figs. 5 and 7) was performed by randomizing the order of speed measurements within each individual trajectory without pooling values from all bacteria. The average change in speed and angular velocity for each bacterium was determined by averaging the absolute value of the difference in speed over all time intervals and all possible pairs of points in a bacterial trajectory. The mean change in speed was calculated and plotted as a function of time interval ($n\Delta t$). To obtain a value for the maximum change in speed, the above analysis was performed on three independently pooled and randomized data sets (inter-track), and the values for each $n\Delta t$ were averaged.

Autocorrelation functions were calculated for each bacterial trajectory using the following equation:

$$RV = \frac{\frac{1}{L-n}\sum_{i=1}^{L-n}(v_i - a)(v_{i+n} - a)}{\frac{1}{L}\sum_{i=1}^{L}(v_m - a)^2}$$

where v_i is the speed of the bacterium in interval i within a video sequence, v_{i+n} is the speed of the bacterium n frames later, Δt is the time interval between frames ($\Delta t = 10$ s), L is the number of points in the trajectory (trajectory length), and a is the average speed for the individual bacterium. The population of autocorrelation functions were averaged and fitted with a single exponential.

The characteristic distance (d) over which intermediate filaments exert their effects on bacterial velocity was determined by calculating the product of the mean speed and the initial autocorrelation decay time constant in vimentin +/+ and vimentin −/− cells.

Angular velocity was measured as the average change in direction over all pairs of adjacent time intervals in a bacterial trajectory. The angle was calculated for each time interval in individual bacterial trajectories as the deviation from the path traveled during the previous interval.

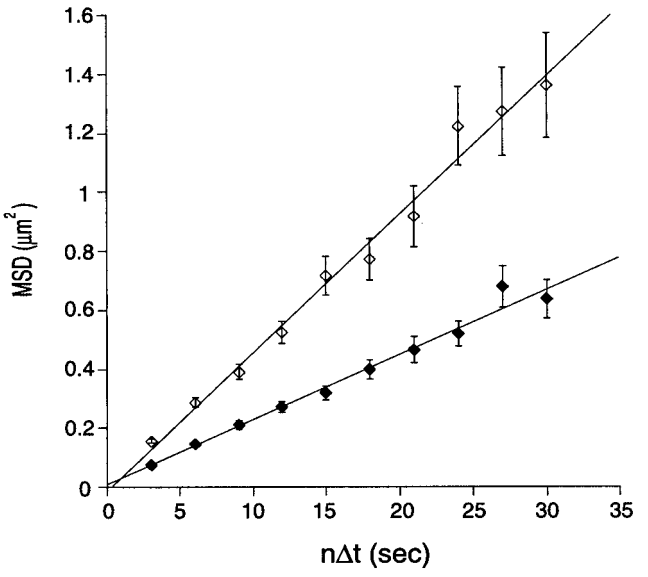

FIGURE 1 Diffusion of *L. monocytogenes* in vimentin +/+ and vimentin −/− fibroblasts. Vimentin −/− (◇) and vimentin +/+ (◆) fibroblasts infected with *L. monocytogenes* strain DP-L1942 (*actA*⁻) were visualized by phase-contrast microscopy with frames recorded every 3 s. The center of 48 bacteria in vimentin +/+ cells and 51 bacteria in vimentin −/− cells was tracked, and the mean-squared displacement (MSD) was calculated from the x, y positions of bacterial trajectories. The mean squared displacement MSD was plotted as a function of ($n\Delta t$), and the diffusion coefficient was derived from the slope of the resulting curve. Error bars are standard error of the mean.

RESULTS

Intermediate filaments constrain movement of bacteria-sized particles

Vimentin is the predominant intermediate filament protein expressed in fibroblasts (Franke and Moll, 1987; Holwell et al., 1997). To determine whether the removal of intermediate filaments would cause an increase in the diffusivity of large objects (1–2 μm in size), we tracked *L. monocytogenes* in cytoplasm of both vimentin +/+ and vimentin −/− fibroblasts. To make measurements of diffusion coefficients that were not confounded by bacterial association with actin, vimentin +/+ and vimentin −/− fibroblasts were infected with *L. monocytogenes* strain DP-L1942, a mutant possessing a large internal in-frame deletion in the *actA* gene (Brundage et al., 1993). These bacteria fail to nucleate actin polymerization at the bacterial surface, and therefore they are unable to undergo actin-based motility or specifically associate with the cytoskeleton. We performed time-lapse video microscopy on infected fibroblasts, acquiring phase-contrast images of a large population of *actA*⁻ bacteria in vimentin +/+ and vimentin −/− host fibroblasts. The mean squared displacement was plotted as a function of time and in both cases was well fit by a straight line, consistent with simple diffusion (Fig. 1). The apparent two-dimensional diffusion coefficient (D), derived from the slope of the resulting curve, was 0.0192 $\mu m^2/s$ in vimentin −/− cells and 0.0096 $\mu m^2/s$ in vimentin +/+ cells. For an ellipsoid the size of *L. monocytogenes* undergoing Brownian motion in an ideal viscous medium, this D would correspond to a viscosity (η) of ~36 cP (Berg, 1993).

The two-fold difference in the observed diffusion coefficient of bacteria in the vimentin +/+ versus the vimentin −/− cells indicated that the local vimentin network constrains the movement of bacteria in host cells and thus imposes a drag force on bacteria and other intracellular objects of comparable size. Similarly, 100-nm beads microinjected into 3T3 fibroblasts derived from a vimentin knockout mouse (Holwell et al., 1997) exhibit a diffusion coefficient that is four-fold greater than the diffusion coefficient of similar beads microinjected into control fibroblasts (Jones et al., 1997). These results, taken together with ours, suggest that the size range over which vimentin networks can constrain the motion of particles is at least 10-fold (0.1 μm to >1 μm).

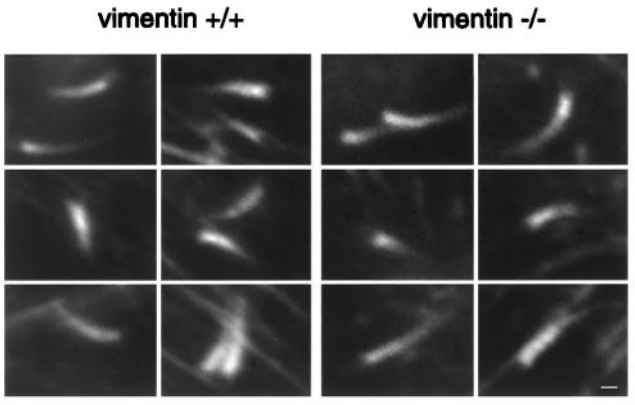

FIGURE 2 Rhodamine-phalloidin staining of *L. monocytogenes* comet tails in vimentin+/+ and vimentin −/− fibroblasts. Six representative comet tails from two different vimentin +/+ host cells and three different vimentin −/− host cells are shown. *L. monocytogenes* tail structure visualized at the level of light microscopy is similar in the vimentin +/+ and vimentin −/− cell lines. Scale bar, 0.5 μm.

Intermediate filaments have no apparent effect on comet tail structures associated with *L. monocytogenes*

Several lines of evidence suggest that intermediate filaments interact with the actin cytoskeleton in various cell types (Svitkina et al., 1996; Correia et al., 1999; Fuchs and Yang, 1999; Herrmann and Aebi, 2000). However, no observable defects in the host cell actin cytoskeleton were detected in the vimentin −/− cell line compared with the vimentin +/+ line (Holwell et al., 1997, and data not shown). To determine specifically whether perturbations in the intermediate filament cytoskeleton had any gross effects on the bacterial comet tail structure, we examined the morphology of actin comet tails associated with motile wild-type *L. monocytogenes* strain 10403S (Bishop and Hinrichs, 1987) in the cytoplasm of vimentin +/+ and vimentin −/− fibroblasts. Fig. 2 shows fluorescence micrographs of representative comet tails from several host cells of each type. The length distribution and overall shape of comet tails associated with *L. monocytogenes* in vimentin +/+ and vimentin −/− cells were indistinguishable.

A two-fold change in bacterial diffusivity has no effect on mean speed of *L. monocytogenes*

The mean speed of *L. monocytogenes* undergoing actin-based motility can be significantly affected by sequence alterations in the protein encoded by *actA* (Smith et al., 1996; Lasa et al., 1997; Skoble et al., 2000) or by changes in the concentration of various cytoskeletal proteins that regulate actin polymerization dynamics (Loisel et al., 1999). However, it is not yet known what governs bacterial speed under normal conditions, nor have the specific effects on speed of changes in the physical environment been described. We therefore measured the mean speed of large populations of wild-type *L. monocytogenes* in the cytoplasm of the vimentin +/+ versus vimentin −/− fibroblasts, determining the position of each bacterium at 10-s intervals over trajectories ranging from 100 to 600 s. The mean speed of bacteria in vimentin +/+ cells was 0.115 μm/s (SD = 0.046, SEM = 0.005, $n = 77$) and 0.113 μm/s (SD = 0.050, SEM = 0.006, $n = 71$) in vimentin −/− cells (Fig. 3 *A*). The distributions of average speeds of the two bacterial populations were similar in shape and were not significantly different by Student's *t*-test.

The magnitude to which speeds vary within individual bacterial trajectories was determined by calculating the standard deviation of speed values within each track. The average standard deviation was 0.040 μm/s (SD = 0.018, SEM = 0.001, $n = 77$) in vimentin +/+ cells and 0.045 μm/s (SD = 0.018, SEM = 0.002, $n = 71$) in vimentin −/− cells (Fig. 3 *B*). These results demonstrate that removal of intermediate filaments has no effect on the mean speed of *L. monocytogenes*, despite the two-fold effect on bacterial diffusion and therefore on environmental drag for moving bacteria.

Bacteria move at intrinsically different speeds in both cell types but display less individuality in cells lacking intermediate filaments

The variation in average speeds for bacteria in either vimentin +/+ and vimentin −/− cells was two orders of magnitude greater (SD ≈ 0.05 μm/s; Fig. 3 *B*) than can be accounted for by tracking error. Are these broad mean speed distributions (Fig. 3 *A*) due to intrinsic differences in speed among individuals or due to large random speed fluctuations within trajectories? If individual trajectories in these populations have a large degree of variation between time intervals, the broad mean speed distributions would reflect random sampling of the variability in speeds within individual trajectories. Alternatively, the broad distribution may be due to individual bacteria in host cells having intrinsically different speeds but relatively little point-to-point variation. In this case, the broad distribution of speeds would be caused by variability among individual trajectories, which may be due either to factors intrinsic to the bacteria or to variations in the cytoplasmic microenvironments through which they move.

To distinguish between these possibilities, we compared our mean speed histograms to histograms generated from a data set where there was no correlation in speed measurements from one point to the next. To generate this uncorrelated data set, we pooled all speed measurements from individual trajectories for each of the real data sets (1931 data points for 77 bacteria in vimentin +/+ cells and 1597 points for 71 bacteria in vimentin −/− cells), randomized the order of the data points in both groups, and reassigned

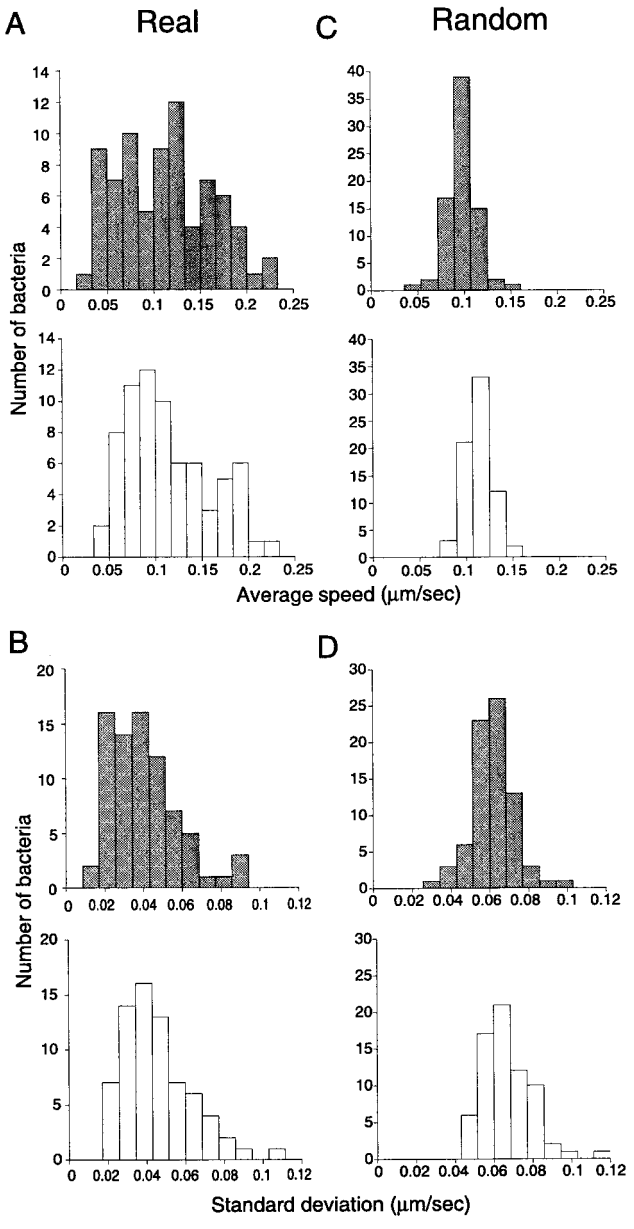

FIGURE 3 Speed and standard deviation distributions of *L. monocytogenes* in vimentin +/+ and vimentin −/− cells. (*A*) Histograms of the average speed of each bacterial trajectory in vimentin +/+ (dark) and vimentin −/− (light) cells. The mean speed for bacteria in vimentin +/+ and vimentin −/− cells is not significantly different by Student's *t*-test. (*B*) Histograms of the standard deviation of the speed distribution within each bacterial trajectory in vimentin+/+ (dark) and vimentin−/− (light) cells. The mean standard deviation for bacteria in vimentin +/+ and vimentin −/− cells is not significantly different by Student's *t*-test. (*C*) Average speed histograms for randomized bacterial trajectories. Speed values from the vimentin +/+ (dark) or vimentin −/− (light) data sets were pooled and randomly reassigned to hypothetical individual bacterial trajectories. Randomized populations show narrower distributions than real populations, indicating that real individual bacteria move at distinct, persistent speeds. (*D*) Histograms of standard deviation of the speed distribution within each randomized bacterial trajectory.

TABLE 1 Comparison of standard deviation of speeds within bacterial trajectories among different bacterial populations

	B			
A	vim +/+ cells	vim −/− cells	vim +/+ randomized	vim −/− randomized
vim +/+ cells	•	=	>>	>>
vim −/− cells		•	>>	>>
vim +/+ randomized			•	=
vim −/− randomized				•

vim, vimentin; =, not significantly different; >>, B very significantly greater than A ($p < 0.001$); < B significantly less than A ($p < 0.05$). Dots represent comparison to self.

the set of randomized speed measurements to individual bacterial trajectories in each of the vimentin +/+ and vimentin −/− populations. We then compared the distributions of average speeds and standard deviations of the actual bacterial populations to those of the randomized data sets. Comparisons were performed for three independent randomized sets with similar results; the distribution of average speeds in a representative randomized set is shown (Fig. 3 *C*). The distributions of average speed for the randomized bacterial trajectories were substantially narrower than the distributions for actual bacterial trajectories in both vimentin +/+ and vimentin −/− cells (compare Fig. 3, *C* and *A*). Conversely, the mean intra-track standard deviation of speeds for randomized bacterial trajectories was significantly larger by Student's *t*-test than that for the actual trajectories of bacteria in either vimentin +/+ and vimentin −/− fibroblasts (compare Fig. 3, *B* and *D*; $p < 0.001$; Table 1). Thus, individual bacteria in both the vimentin +/+ and vimentin −/− cells move at intrinsically different speeds.

The randomization analysis did reveal a significant difference in behavior of bacteria in vimentin +/+ versus vimentin −/− cells. The mean speed of randomized bacterial trajectories in vimentin +/+ cells was only 0.097 μm/s (SD = 0.015, SEM = 0.001, $n = 77$), compared with 0.115 μm/s (SD = 0.014, SEM = 0.002, $n = 71$) in vimentin −/− cells (Fig. 3 *C*). The mean speed for randomized bacterial trajectories in the vimentin +/+ population was significantly lower than the mean speed of actual bacteria in vimentin +/+ cells by Student's *t*-test (Table 2; Fig. 3, *A*

TABLE 2 Comparison of average speeds among different bacterial populations

	B			
A	vim +/+ cells	vim −/− cells	vim +/+ randomized	vim −/− randomized
vim +/+ cells	•	=	<	=
vim −/− cells		•	<	=
vim +/+ randomized			•	>>
vim −/− randomized				•

See Table 1 for explanation of symbols.

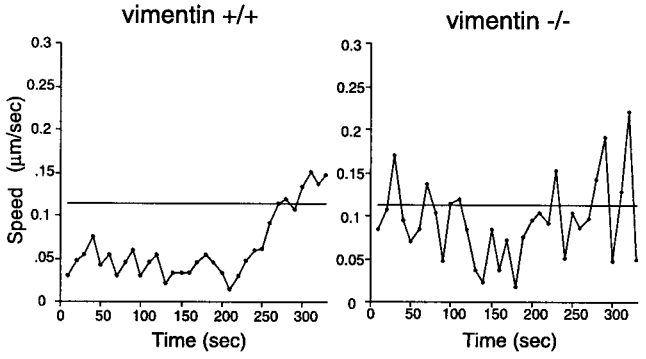

FIGURE 4 Speed fluctuations in vimentin +/+ and vimentin −/− fibroblasts. Speed traces of a representative bacterium from a vimentin +/+ (*left*) and a vimentin −/− cell (*right*). The horizontal line represents the mean speed for the vimentin +/+ (*left*) or vimentin −/− (*right*) population of bacteria. The standard deviation for both traces is similar.

and C; $p = 0.01$). In contrast, the value of the mean speed for randomized bacterial trajectories in vimentin −/− cells is similar to the value for actual bacteria (Table 2; Fig. 3, *A* and *C*). These data suggest that the distribution of mean speeds in the vimentin +/+ cells is weighted by a subpopulation of bacteria moving at atypically fast but constant speeds. Therefore, although distributions of average speed for bacteria in both vimentin+/+ and vimentin −/− cells have a large variance, the cause of this variance is not the same in the two cases. Bacteria moving in the presence of intracellular intermediate filaments have a greater tendency to exhibit persistent differences in average speed among individuals in the population, whereas bacteria moving in the absence of intermediate filaments tend to display less individuality in average speed.

Speed fluctuations are greater in cells lacking intermediate filaments

To specifically determine the effects of changing the cytoarchitecture on speed fluctuations, we examined the speed as a function of time for all bacterial trajectories in the vimentin +/+ and vimentin −/− cells. A representative example from each population is shown in Fig. 4. The speed of the bacterium in the vimentin −/− cell fluctuated dramatically above and below the mean speed of the population, represented by the horizontal line. The majority (89%) of trajectories in the vimentin −/− population displayed these large speed fluctuations. In contrast, the speed for the bacterium in the vimentin +/+ cell tended to persist below the population mean with less severe point-to-point variability. Note that movement of this bacterium started slow, then gradually increased in speed. Other individual traces persist above the mean velocity. The standard deviations of speeds for both traces were similar (Fig. 4), representative of the observation that the distributions of standard deviations for both populations were similar (Fig. 3 *B*). But

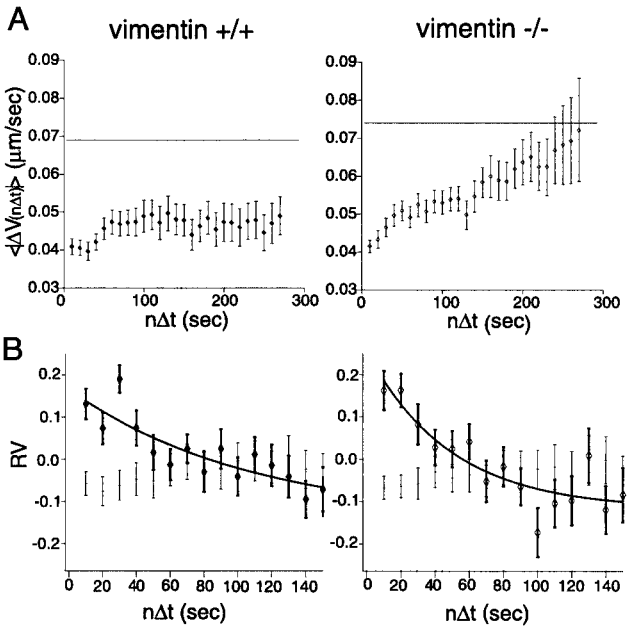

FIGURE 5 Time-dependent changes in speed for bacteria in vimentin +/+ and vimentin −/− cells. (*A*) The mean absolute value of the change in speed $\langle|\Delta V|\rangle$ as a function of time interval ($n\Delta t$) for all bacteria in vimentin +/+ and vimentin −/− fibroblasts. The horizontal line represents the mean change in speed for pooled, randomized trajectories. (*B*) Speed autocorrelation decay for bacteria in vimentin +/+ and vimentin −/− cells (*dark bars*). Autocorrelation functions (RV) were calculated for each individual, and the populations of autocorrelation functions were averaged. Dashes represent average change in speed for the same data set with the order of speed measurements randomized within each trajectory (*light bars*). Curves shown are best-fit single exponential determined by least-squares analysis. Error bars are standard error of the mean.

strikingly, these traces suggested that there was a greater degree of rapid variation in speed for bacteria in cells lacking vimentin networks than for corresponding bacteria in normal host cells.

Persistence of bacterial speed is shortened in cells lacking intermediate filaments

To examine the time dependence of speed fluctuations, we calculated the change in speed between all possible pairs of measurements for all bacteria in the vimentin +/+ and vimentin −/− populations. The mean change in speed for the vimentin +/+, vimentin −/−, and randomized data sets was plotted as a function of time interval ($n\Delta t$) (Fig. 5 *A*). The horizontal line represents the mean change in speed calculated from pooled, randomized data (Fig. 3 *C*), which does not vary with time interval ($\langle|\Delta V_{n\Delta t}|\rangle = 0.069$ μm/s for pooled, randomized bacterial trajectories in vimentin +/+ cells and 0.074 μm/s for pooled, randomized bacterial trajectories in vimentin −/− cells) (Fig. 5 *A*). The speed change for trajectories of bacteria in vimentin −/− cells approached the average for the pooled randomized data set

within 200 s, whereas this average change could not be approached for intervals greater than 300 s for bacteria in vimentin +/+ cells. Thus, intermediate filaments limit the magnitude of fluctuations in bacterial speed and prolong speed persistence. In addition, the variance in the speed measurements for bacteria in vimentin −/− cells increases at larger time intervals ($n\Delta t$) but remains relatively constant for bacteria in vimentin +/+ cells, suggesting that speed changes in vimentin −/− cells (but not vimentin +/+ cells) have a significant random component.

The observation that the value of $\langle|\Delta V_{n\Delta t}|\rangle$ for bacteria moving in vimentin +/+ cells does not approach the maximum theoretical value as derived from the randomized population over at least 300 s indicates that the average speed changes within each individual track are small compared with the variability present in the whole population. To examine this possibility more directly, we performed a second type of randomization analysis, where the order of speed measurements within each track was randomized without first pooling all the tracks in each population. With this intra-track randomized population, we found that the average value of $\langle|\Delta V_{n\Delta t}|\rangle$ for all time intervals is significantly smaller for bacteria moving in vimentin +/+ cells than for bacteria moving in vimentin −/− cells (0.040 μm/s vs. 0.058 μm/s; $p < 0.001$ by Student's *t*-test). Thus, the intrinsically different speeds for different bacteria are more persistent in vimentin +/+ cells than in vimentin −/− cells.

To explore quantitatively the time dependence of speed persistence in both cell types, we calculated the correlation between successive speed measurements for each individual in our bacterial populations. Autocorrelation functions (RV) were calculated for each bacterium normalized to the individual's average speed and visually examined separately. There were no major outliers in either the vimentin +/+ or vimentin −/− data sets. Therefore, the population of autocorrelation functions were averaged and fitted with a single exponential. The average autocorrelation decay is faster for bacteria in the vimentin −/− cells, although as expected, both autocorrelation functions showed appreciable persistence when compared with equivalent autocorrelations calculated from the randomized populations (Fig. 5 *B*). The autocorrelation decay constant ($t_{1/2}$) was 75 s for bacteria in vimentin +/+ cells and 34 s for bacteria in vimentin −/− cells. At our shortest time interval (10 s) the autocorrelations had already fallen to a relatively low value of 0.2, indicating that speed fluctuations were also influenced by a fast-acting process with a time constant of less than 10 s, which we cannot distinguish with our relatively long sampling intervals. Similarly, our data cannot address any processes that take place over times of greater than several hundred seconds. However, these data do indicate that the maintenance of speed over periods of tens of seconds is strongly influenced by the drag imposed by intermediate filaments, such that the presence of intermediate filaments extends the persistence of speed by about two-fold. Using the measured time constants, we estimated that the characteristic distance over which the intermediate filament network exerts its effect on bacterial speed is 4.5 μm, similar to the length of the actin comet tail.

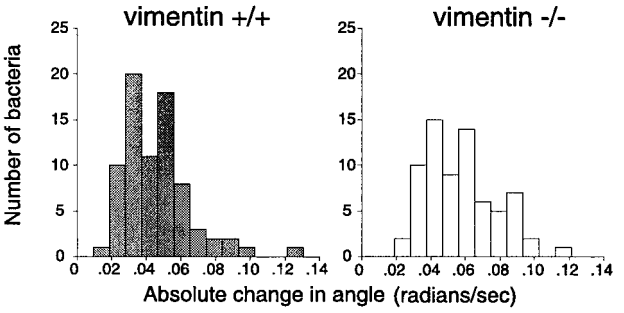

FIGURE 6 Angular change distributions in vimentin +/+ and vimentin −/− cells. Histograms of the average of the absolute change in angle between adjacent time intervals for bacteria in vimentin +/+ (*shaded bars*) and vimentin −/− (*open bars*). The mean change is significantly larger for bacteria in vimentin +/+ cells than for those in vimentin −/− cells by Student's *t*-test ($p < 0.001$).

Angular deviations of *L. monocytogenes* are greater in cells lacking intermediate filaments

Because we found that the presence of a vimentin network dampens fluctuations in speed and promotes persistence of speed from one moment to the next, we hypothesized that this dampening effect might also manifest itself on an independent motility parameter, the bacterial propensity to turn. We determined the average absolute angle change over each adjacent pair of 10-s intervals for each bacterial trajectory and examined the distributions of these average angular velocities for bacterial populations in vimentin +/+ and vimentin −/− cells (Fig. 6). For the bacterial population in vimentin +/+ cells, mean angular velocity was 0.046 radians/s (SD = 0.019, SEM = 0.002, $n = 77$). The mean angular velocity for bacteria in vimentin −/− cells was 0.058 radians/s (SD = 0.021, SEM = 0.003, $n = 71$). This value was significantly larger than the mean angular velocity for bacteria in vimentin +/+ cells by Student's *t*-test ($p < 0.001$). Combined with the results shown in Fig. 5, these data strongly support the idea that intermediate filaments significantly dampen fluctuations in bacterial velocity both parallel to and perpendicular to the direction of movement.

Because translational velocity fluctuations are dampened in the presence of vimentin, it seemed likely that fluctuations in angular velocity might be too. We therefore calculated the mean change in angular velocity between all possible pairs of intervals for all trajectories (ΔS) and plotted these data as a function of time interval ($n\Delta t$) (Fig. 7 *A*). Although the value of the average change in angular velocity for pooled randomized data sets is much higher for vimentin −/− cells, the time of approach to that value

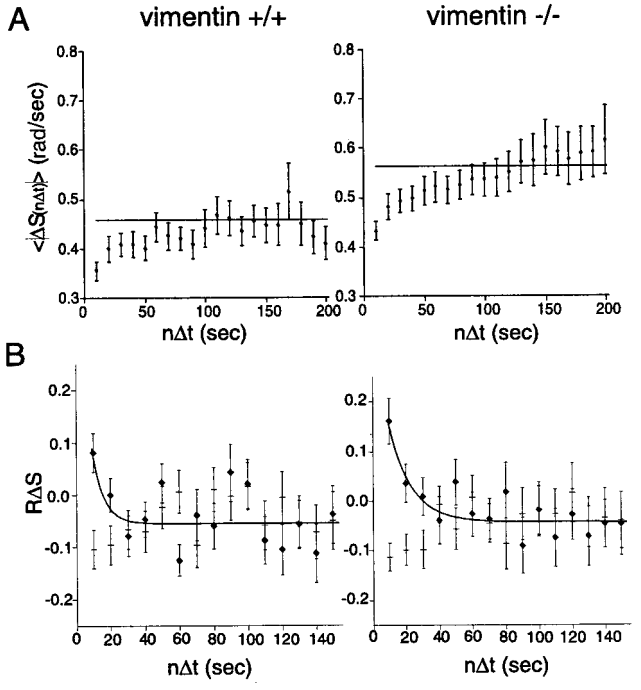

FIGURE 7 Time-dependent change in angular speed for bacteria in vimentin +/+ and vimentin −/− fibroblasts. (*A*) The mean average change in angle ($\langle|\Delta S|\rangle$) was calculated and plotted as a function of time interval ($n\Delta t$). The horizontal line represents the mean change in angle for the pooled, randomized trajectories derived from the population of vimentin +/+ cells (*left*) and vimentin −/− cells (*right*). (*B*) Angular velocity autocorrelation decay ($\langle R\Delta S\rangle$) for bacteria in vimentin +/+ (*left*) and vimentin −/− cells (*right*) as a function of time interval ($n\Delta t$) (*heavy bars*). Dashes represent average change in angle for data points that were randomized within the individual trajectories (*light bars*). Curves shown are best-fit single exponential determined by least-squares analysis. Error bars are standard error of the mean.

occurred within the first 120 s for bacteria in both vimentin +/+ and vimentin −/− cells. Additionally, we calculated the mean autocorrelation coefficients ($R\Delta S$) and plotted them as a function of time interval ($n\Delta t$) (Fig. 7 *B*). As with speed, the angular velocity autocorrelation in both populations showed appreciable persistence when compared with autocorrelations calculated from tracks that had been randomized without pooling. Surprisingly, the angular velocity autocorrelation decay constant as calculated by fitting the curves to a single exponential was significantly longer for the vimentin −/− cells than for the vimentin +/+ cells (10.5 s vs. 5.3 s). However, because our shortest measurement intervals were 10 s, we cannot reliably interpret these very short fitted time constants.

DISCUSSION

L. monocytogenes is a kinematic probe of subcellular architecture

In this report, we have shown that *L. monocytogenes* can be used as a moving probe of cytoskeletal architecture. This system has several advantages over stationary probes. First, passive inert probes are often restricted to regions of the cell where there is sufficient volume to accommodate them. As a result, the cytoarchitecture of the perinuclear region of cells is well characterized, but other regions such as the lamellipodium and cellular projections are not. A self-propelled moving probe such as *L. monocytogenes* can explore the structural properties of all regions of the host cell cytoplasm. Second, a moving probe allows one to study the time dependence and persistence of effects of the subcellular environment on directed movement. These kinematic parameters cannot be examined by tracking Brownian movement alone. We have found that several types of variations in *L. monocytogenes* movement are well correlated with the presence or absence of an intermediate filament meshwork. To extend these results, we plan to use the motility properties of *L. monocytogenes* to map out changes in cytoskeletal organization within subregions of single cells.

Intermediate filament networks are correlated with changes in intracellular actin-based bacterial motility

It is generally accepted that intermediate filaments are important for maintaining mechanical stability, cytoskeletal integrity, and overall cell morphology (Janmey, 1991; Wang et al., 1993; Ingber et al., 1994; Sarria et al., 1994; Lloyd et al., 1995; Goldman et al., 1996; Eckes et al., 1998). Goldman et al. (1996) demonstrated that the disassembly of vimentin networks in fibroblasts disrupted the organization of the actin and microtubule cytoskeleton, leading to the conclusion that intermediate filament networks are required for cytoskeletal organization and proper cell morphology. Surprisingly, vimentin −/− mice develop and reproduce normally and have no discernibly unusual characteristics (Colucci-Guyon et al., 1994), and fibroblasts prepared from these mice have apparently normal growth and morphology (Holwell et al., 1997; but contrast Eckes et al., 1998). It is possible that the constraints of development have forced the acquisition of compensatory adaptations in vimentin −/− mice. However, we find no difference in the average speed of *L. monocytogenes* actin-based motility in equivalent cell lines derived from isogenic vimentin +/+ and vimentin −/− mice, even though bacterial speed is strongly affected by changes in the concentration of many of the protein factors involved in regulating actin dynamics (Loisel et al., 1999). Thus, any compensatory adaptations that have occurred are unlikely to directly affect actin dynamics or organization. Furthermore, the gross changes in cytoplasmic viscosity have clearly not been compensated, because we can measure a two-fold increase in the diffusion coefficient for *L. monocytogenes* in these cells. Therefore, it seems more likely that the behavioral changes that we do detect are due to the mechanical differences in the cytoplasm of these

two cell lines. Ideally, we would like to be able to ascribe the observed mechanical differences solely to the presence or absence of intermediate filaments by expressing vimentin at wild-type levels in the vimentin −/− cell line and determining whether normal behavior had been restored. Unfortunately, Holwell et al. (1997) showed that different cell lines generated by transfection of parental vimentin −/− cells with a vimentin transgene express very different levels of vimentin. Furthermore, expression of genes under the control of the CMV promoter used in these transfections produces highly variable levels of expression among individual cells in a clonal population (Robbins et al., 1999; Li et al., 1992). Because of the high degree of variability of vimentin expression in transfected cells, we chose not to use such cells in our study. Because our quantitative analysis requires the comparison of behavior of many individual bacteria in different host cells, these sources of variability would make the results of such an experiment uninterpretable.

The simplest interpretation of our results is that the presence of an intermediate filament network lessens fluctuations in bacterial speed, exerting effects over distances of several microns, comparable to the typical length of *L. monocytogenes* comet tails. How might intermediate filaments suppress variability in movement associated with the actin tail? One possibility is a tail entanglement model where the bacterium and its tightly associated comet tail (Gerbal et al., 2000a; Kuo and McGrath, 2000) can undergo Brownian motion that is superimposed on net directed movement. Intermediate filaments interacting with the comet tail may dampen the Brownian motion of the bacterium/tail system, therefore minimizing fluctuations in speed measured for bacteria. The dampening may occur by a mechanical or biochemical mechanism, or combination of both. We have shown that the diffusion of the bacterium in cytoplasm is decreased two-fold in the presence of intermediate filaments, suggesting that the bacterium itself can be physically entangled in the intermediate filament network. Because the tightly associated comet tail is approximately the same diameter as the bacterium, we expect that the physical constraints imposed by intermediate filaments would be of similar magnitude for the tail. Alternatively, molecular interactions may cross-bridge intermediate filaments to the actin comet tail. Several proteins cross-link intermediate filaments to actin filaments, including bullous pemphigoid antigen 1 (BPAG1), fimbrin, calponin, and plectin (reviewed in Coulombe et al., 2000). The dense intermediate filament network, cross-linked to actin filaments in the comet tail, may serve as a structural scaffold from which the comet tail elongates to push the bacterium. If molecular cross-linkers mediate the dampening of fluctuations in bacterial velocity by attaching the actin comet tail to intermediate filament networks, *L. monocytogenes* is predicted to undergo greater fluctuations in cells where molecular cross-linkers are absent. In contrast, if the interaction is primarily mechanical, the loss of specific actin-intermediate filament cross-linking proteins should have little effect. It may be possible, therefore, to distinguish whether the dampening effect we observe is due to a molecular or a physical interaction.

Influence of subcellular environment on force generation for *L. monocytogenes* movement

The Reynolds number (ratio of inertial to viscous forces) for *L. monocytogenes* movement in fibroblasts is $\sim 10^{-9}$. At such low Reynolds number, speed is a function of the net sum of forces acting on the object at that moment in time (Purcell, 1977). The force for bacterial movement is thought to result from the potential energy of actin polymerization itself (Theriot et al., 1992; Sanger et al., 1992). Based on the amount of free energy available for chemomechanical energy transduction, thermodynamic laws can set theoretical limits on the amount of force that actin polymerization can generate for movement (Hill and Kirschner, 1982), but in the absence of a kinetic model they cannot predict speed. Because actin polymerization occurs exclusively at or near the bacterial surface (Sanger et al., 1992) and bacterial movement occurs at the same rate as net actin polymerization (Theriot et al., 1992), it seems likely that overall speed is limited by the rate at which filaments can elongate at the bacterial surface. In a model system for *L. monocytogenes* motility reconstituted from purified cytoskeletal proteins, actin at a concentration of 7.4 μM supports bacterial movement speeds no greater than 0.05 μm/s (Loisel et al., 1999). Free polymerization of an unloaded actin filament is diffusion limited and occurs at a net rate of $\sim 10\ \mu M^{-1}\ s^{-1}$ (Pollard et al., 2000), corresponding to an expected elongation rate of $\sim 0.2\ \mu$m/s for actin at 7.4 μM. What accounts for this speed discrepancy?

One possible simple kinetic model, known as the inelastic Brownian ratchet, suggests that actin polymerization may serve to rectify the diffusive movement of the bacterium (Peskin et al., 1993). This model makes two testable predictions: 1) the size of thermal fluctuations of bacterial position should be greater than the size of the actin monomer, and 2) changing the bacterial diffusion coefficient should result in a change in the net velocity of the bacterium. Recently, Kuo and McGrath (2000) used high-resolution laser tracking to show that fluctuations in position of *L. monocytogenes* in COS7 cells are smaller than the intercalation size of actin monomer, inconsistent with one prediction of the inelastic Brownian ratchet model. In this report, we have shown that, although the macroscopic diffusion coefficient of *L. monocytogenes* doubles in vimentin −/− cells, the mean speed remains the same, negating the second prediction of this model. We have studied the effects of the subcellular environment on *L. monocytogenes* movement at a micron scale, complementary to the nanometric measurements of Kuo and McGrath (2000). Together, these

studies contradict the predictions of a class of models where bacterial diffusion is rate limiting for velocity (Peskin et al., 1993).

Other classes of kinetic models, known as elastic Brownian ratchets, suggest that thermal movements of system components other than the bacterium may open up space for monomer intercalation. For example, thermal bending of filaments may be sufficient (Mogilner and Oster, 1996) or compliance of the cross-links holding the filaments together in the comet tail. In this class of models, predictions for bacterial speed depend strongly on the exact set of assumptions and can vary significantly depending on the assumed bending modulus of the filaments, the compliance of the postulated links, the number of filaments involved in pushing, the mean filament separation, the angle of incidence between the filament and the bacterial surface, etc. (Mogilner and Oster, 1996). In all cases, net speed must depend on the balance between pushing forces and forces that resist bacterial movement, which include environmental drag and the strength of attachment between the moving bacterium and the stationary filaments in the comet tail (Gerbal et al., 2000a).

Our present results cannot distinguish the magnitudes of these various forces contributing to net bacterial movement, but do place constraints on the relationships among them. We find that a two-fold change in environmental drag has no effect on net speed, which must mean either that 1) the influence of environmental drag is entirely negligible compared with the influence of other resistive forces or 2) the system compensates for an increase in environmental drag with a concomitant increase in propulsive force. This second possibility is supported by the observation that bacteria slowed down by encountering environmental obstacles will accumulate a higher local density of actin filaments in the comet tail, generating concomitantly greater force (Fung and Theriot, 1998). This force-coupling relationship is independent of the microscopic mechanism of force generation and is entirely consistent with a mathematical framework where the comet tail is treated as a continuous gel that can undergo elastic compression (Gerbal et al., 2000a). In this framework, variations in speed may be due to variations in local compression of the comet tail. Given our result that intermediate filaments interact with the comet tail in such a way as to minimize fluctuations in net speed, it is possible that intermediate filaments intercalate in the actin gel of the tail to give it more uniform elastic properties. This type of effect, mechanistically distinct from the tail entanglement outlined above, could be detected by direct measurements of elastic compliance of comet tails (Gerbal et al., 2000b) formed in the presence or absence of vimentin.

Biophysical models make specific testable predictions about how certain perturbations should affect bacterial speed, and provide a useful framework for designing experiments to address how actin polymerization is coupled to force generation and *L. monocytogenes* motility. However, it is important to note that each of these models make necessary simplifying assumptions and individually cannot fully account for the complexities of *L. monocytogenes* movement. Furthermore, they are not mutually exclusive. In reality, the biophysical mechanism of actin-based bacterial motility may involve aspects of several different theoretical models. Direct biophysical experimentation, together with the abundance of available molecular data can address which aspects of these models, if any, explain how actin polymerization generates force for *L. monocytogenes* movement.

We are grateful to Robert Evans for kindly providing the cell lines for this study. We thank Katherine Luby-Phelps for helpful discussions and advice on diffusion measurements and Gilbert Chu for suggesting the randomization analysis. Finally, we thank Jennifer Robbins, James Nelson, Scot Kuo, Dan Fletcher, and Li Kung for critiquing the manuscript.

This work was supported by National Institutes of Health grant R01AI36929 and a Fellowship for Science and Engineering from the David and Lucile Packard Foundation to J.A.T. P.A.G is supported by PHS grant CA09302, awarded by the National Cancer Institute to the Stanford University Cancer Biology Program.

REFERENCES

Berg. H. 1993. Random Walks in Biology. Princeton University Press, Princeton, NJ.

Bishop, D. K., and D. J. Hinrichs. 1987. Adoptive transfer of immunity to *Listeria monocytogenes*: the influence of in vitro stimulation on lymphocyte subset requirements. *J. Immunol.* 139:2005–2009.

Brundage, R. A., G. A. Smith, A. Camilli, J. A. Theriot, and D. A. Portnoy. 1993. Expression and phosphorylation of the *Listeria monocytogenes* ActA protein in mammalian cells. *Proc. Natl. Acad. Sci. U.S.A.* 90: 11890–11894.

Cameron, L. A., P. A. Giardini, F. S. Soo, and J. A. Theriot. 2000. Secrets of actin-based motility revealed by a bacterial pathogen. *Nat. Rev. Mol. Cell Biol.* 1:110–119.

Colucci-Guyon, E., M. M. Portier, I. Dunia, D. Paulin, S. Pournin, and C. Babinet. 1994. Mice lacking vimentin develop and reproduce without an obvious phenotype. *Cell.* 79:679–694.

Correia, I., D. Chu, Y. H. Chou, R. D. Goldman, and P. Matsudaira. 1999. Integrating the actin and vimentin cytoskeletons: adhesion-dependent formation of fimbrin-vimentin complexes in macrophages. *J. Cell Biol.* 146:831–842.

Coulombe, P. A., O. Bousquet, L. Ma, S. Yamada, and D. Wirtz. 2000. The 'ins' and 'outs' of intermediate filament organization. *Trends Cell Biol.* 10:420–428.

Dabiri, G. A., J. M. Sanger, D. A. Portnoy, and F. S. Southwick. 1990. *Listeria monocytogenes* moves rapidly through the host-cell cytoplasm by inducing directional actin assembly. *Proc. Natl. Acad. Sci. U.S.A.* 87:6068–6072.

David, V., E. Gouin, M. V. Troys, A. Grogan, A. W. Segal, C. Ampe, and P. Cossart. 1998. Identification of cofilin, coronin, Rac and capZ in actin tails using a Listeria affinity approach. *J. Cell Sci.* 111:2877–2884.

Eckes, B., D. Dogic, E. Colucci-Guyon, N. Wang, A. Maniotis, D. Ingber, A. Merckling, F. Langa, M. Aumailley, A. Delouvee, V. Koteliansky, C. Babinet, and T. Krieg. 1998. Impaired mechanical stability, migration and contractile capacity in vimentin-deficient fibroblasts. *J. Cell Sci.* 111:1897–1907.

Franke, W. W., and R. Moll. 1987. Cytoskeletal components of lymphoid organs. I. Synthesis of cytokeratins 8 and 18 and desmin in subpopulations of extrafollicular reticulum cells of human lymph nodes, tonsils, and spleen. *Differentiation.* 36:145–163.

Fuchs, E., and Y. Yang. 1999. Crossroads on cytoskeletal highways. *Cell.* 98:547–550.

Fung, D. C., and J. A. Theriot. 1998. Movement of bacterial pathogens driven by actin polymerization. *In* Motion Analysis of Living Cells. D.R. Solls and D. Wessels, editors. John Wiley and Sons, Inc., New York, NY. 157–176.

Gerbal, F., P. Chaikin, Y. Rabin, and J. Prost. 2000a. An elastic analysis of Listeria monocytogenes propulsion. *Biophys. J.* 79:2259–2275.

Gerbal, F., V. Laurent, A. Ott, M. F. Carlier, P. Chaikin, and J. Prost. 2000b. Measurement of the elasticity of the actin tail of Listeria monocytogenes. *Eur. Biophys. J.* 29:134–140.

Goldman, R. D., S. Khuon, Y. H. Chou, P. Opal, and P. M. Steinert. 1996. The function of intermediate filaments in cell shape and cytoskeletal integrity. *J. Cell Biol.* 134:971–983.

Goulian, M., and S. M. Simon. 2000. Tracking single proteins within cells. *Biophys. J.* 79:2188–2198.

Herrmann, H., and U. Aebi. 2000. Intermediate filaments and their associates: multi-talented structural elements specifying cytoarchitecture and cytodynamics. *Curr. Opin. Cell Biol.* 12:79–90.

Hill, T. L., and M. W. Kirschner. 1982. Bioenergetics and kinetics of microtubule and actin filament assembly-disassembly. *Int. Rev. Cytol.* 78:1–125.

Holwell, T. A., S. C. Schweitzer, and R. M. Evans. 1997. Tetracycline regulated expression of vimentin in fibroblasts derived from vimentin null mice. *J. Cell Sci.* 110:1947–1956.

Ingber, D. E., L. Dike, L. Hansen, S. Karp, H. Liley, A. Maniotis, H. McNamee, D. Mooney, G. Plopper, J. Sims, and et al. 1994. Cellular tensegrity: exploring how mechanical changes in the cytoskeleton regulate cell growth, migration, and tissue pattern during morphogenesis. *Int. Rev. Cytol.* 150:173–224.

Janmey, P. A. 1991. Mechanical properties of cytoskeletal polymers. *Curr. Opin. Cell Biol.* 3:4–11.

Janson, L. W., K. Ragsdale, and K. Luby-Phelps. 1996. Mechanism and size cutoff for steric exclusion from actin-rich cytoplasmic domains. *Biophys. J.* 71:1228–1234.

Jones, J. D., G. K. Ragsdale, A. Rozelle, H. L. Yin, and K. Luby-Phelps. 1997. Diffusion of vesicle-sized particles in living cells is restricted by intermediate filaments. *Mol. Biol. Cell.* 8:174a.

Kuo, S. C., and J. L. McGrath. 2000. Steps and fluctuations of *Listeria monocytogenes* during actin-based motility. *Nature.* 407:1026–1029.

Lasa, I., E. Gouin, M. Goethals, K. Vancompernolle, V. David, J. Vandekerckhove, and P. Cossart. 1997. Identification of two regions in the N-terminal domain of ActA involved in the actin comet tail formation by *Listeria monocytogenes*. *EMBO J.* 16:1531–1540.

Li, M., P. A. Hantzopoulos, D. Banerjee, S. C. Zhao, B. I. Schweitzer, E. Gilboa, and J. R. Bertino. 1992. Comparison of the expression of a mutant dihydrofolate reductase under control of different internal promoters in retroviral vectors. *Hum. Gene Ther.* 3:381–390.

Loisel, T. P., R. Boujemaa, D. Pantaloni, and M. F. Carlier. 1999. Reconstitution of actin-based motility of *Listeria* and *Shigella* using pure proteins. *Nature.* 401:613–616.

Luby-Phelps, K. 1994. Physical properties of cytoplasm. *Curr. Opin. Cell Biol.* 6:3–9.

Luby-Phelps, K. 2000. Cytoarchitecture and physical properties of cytoplasm: volume, viscosity, diffusion, intracellular surface area. *Int. Rev. Cytol.* 192:189–221.

Luby-Phelps, K., P. E. Castle, D. L. Taylor, and F. Lanni. 1987. Hindered diffusion of inert tracer particles in the cytoplasm of mouse 3T3 cells. *Proc. Natl. Acad. Sci. U.S.A.* 84:4910–4913.

Luby-Phelps, K., and D. L. Taylor. 1988. Subcellular compartmentalization by local differentiation of cytoplasmic structure. *Cell. Motil. Cytoskel.* 10:28–37.

Luby-Phelps, K., D. L. Taylor, and F. Lanni. 1986. Probing the structure of cytoplasm. *J. Cell Biol.* 102:2015–2022.

May, R. C., M. E. Hall, H. N. Higgs, T. D. Pollard, T. Chakraborty, J. Wehland, L. M. Machesky, and A. S. Sechi. 1999. The Arp2/3 complex is essential for the actin-based motility of *Listeria monocytogenes*. *Curr. Biol.* 9:759–762.

Mogilner, A., and G. Oster. 1996. Cell motility driven by actin polymerization. *Biophys. J.* 71:3030–3045.

Mounier, J., A. Ryter, M. Coquis-Rondon, and P. J. Sansonetti. 1990. Intracellular and cell-to-cell spread of *Listeria monocytogenes* involves interaction with F-actin in the enterocytelike cell line Caco-2. *Infect. Immun.* 58:1048–1058.

Nanavati, D., F. T. Ashton, J. M. Sanger, and J. W. Sanger. 1994. Dynamics of actin and alpha-actinin in the tails of *Listeria monocytogenes* in infected PtK2 cells. *Cell. Motil. Cytoskel.* 28:346–358.

Peskin, C. S., G. M. Odell, and G. F. Oster. 1993. Cellular motions and thermal fluctuations: the Brownian ratchet. *Biophys. J.* 65:316–324.

Pollard, T. D. 1986. Rate constants for the reactions of ATP- and ADP-actin with the ends of actin filaments. *J. Cell Biol.* 103:2747–2754.

Pollard, T. D., L. Blanchoin, and R. D. Mullins. 2000. Molecular mechanisms controlling actin filament dynamics in nonmuscle cells. *Annu. Rev. Biophys. Biomol. Struct.* 29:545–576.

Purcell. 1977. Life at low Reynolds number. *Am. J. Phys.* 45:3–11.

Qian, H., M. P. Sheetz, and E. L. Elson. 1991. Single particle tracking: analysis of diffusion and flow in two-dimensional systems. *Biophys. J.* 60:910–921.

Robbins, J. R., A. I. Barth, H. Marquis, E. L. de Hostos, W. J. Nelson, and J. A. Theriot. 1999. *Listeria monocytogenes* exploits normal host cell processes to spread from cell to cell. *J. Cell Biol.* 146:1333–1350.

Sanger, J. M., J. W. Sanger, and F. S. Southwick. 1992. Host cell actin assembly is necessary and likely to provide the propulsive force for intracellular movement of *Listeria monocytogenes*. *Infect. Immun.* 60: 3609–3619.

Sarria, A. J., J. G. Lieber, S. K. Nordeen, and R. M. Evans. 1994. The presence or absence of a vimentin-type intermediate filament network affects the shape of the nucleus in human SW-13 cells. *J. Cell Sci.* 107:1593–1607.

Saxton, M. J. 1997. Single-particle tracking: the distribution of diffusion coefficients. *Biophys. J.* 72:1744–1753.

Skoble, J., D. A. Portnoy, and M. D. Welch. 2000. Three regions within ActA promote Arp2/3 complex-mediated actin nucleation and *Listeria monocytogenes* motility. *J. Cell Biol.* 150:527–538.

Smith, G. A., J. A. Theriot, and D. A. Portnoy. 1996. The tandem repeat domain in the *Listeria monocytogenes* ActA protein controls the rate of actin-based motility, the percentage of moving bacteria, and the localization of vasodilator-stimulated phosphoprotein and profilin. *J. Cell Biol.* 135:647–660.

Svitkina, T. M., A. B. Verkhovsky, and G. G. Borisy. 1996. Plectin sidearms mediate interaction of intermediate filaments with microtubules and other components of the cytoskeleton. *J. Cell Biol.* 135: 991–1007.

Theriot, J. A., T. J. Mitchison, L. G. Tilney, and D. A. Portnoy. 1992. The rate of actin-based motility of intracellular *Listeria monocytogenes* equals the rate of actin polymerization. *Nature.* 357:257–260.

Theriot, J. A., J. Rosenblatt, D. A. Portnoy, P. J. Goldschmidt-Clermont, and T. J. Mitchison. 1994. Involvement of profilin in the actin-based motility of *L. monocytogenes* in cells and in cell-free extracts. *Cell.* 76:505–517.

Tilney, L. G., and D. A. Portnoy. 1989. Actin filaments and the growth, movement, and spread of the intracellular bacterial parasite, *Listeria monocytogenes*. *J. Cell Biol.* 109:1597–1608.

Wang, N., J. P. Butler, and D. E. Ingber. 1993. Mechanotransduction across the cell surface and through the cytoskeleton. *Science.* 260: 1124–1127.

Welch, M. D., A. Iwamatsu, and T. J. Mitchison. 1997. Actin polymerization is induced by Arp2/3 protein complex at the surface of *Listeria monocytogenes*. *Nature.* 385:265–269.

Yamada, S., D. Wirtz, and S. C. Kuo. 2000. Mechanics of living cells measured by laser tracking microrheology. *Biophys. J.* 78:1736–1747.